https://doi.org/10.5194/egusphere-2025-4460 Preprint. Discussion started: 18 November 2025 © Author(s) 2025. CC BY 4.0 License.

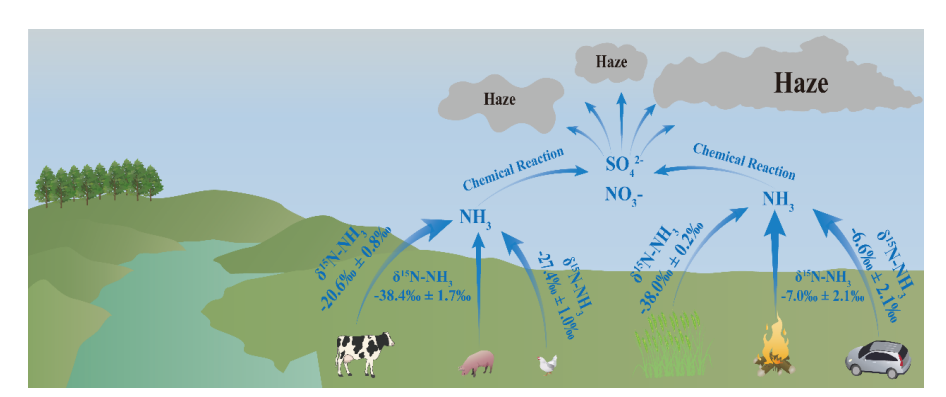




- 1 Measurement report: Nitrogen Isotope (δ¹⁵N) Signatures of Ammonia Emissions
- 2 from Livestock Farming: Implications for Source Apportionment of Haze
- 3 Pollution
- 4 Jinhan Wang¹, Zhaojun Nie¹, Yupeng Zhang¹, Xiaolei Jie^{1,2}, Haiyang Liu¹, Peng
- 5 Zhao^{1,2,3}, Hongen Liu^{1,2,3}
- 6 College of Resources and Environment, Henan Agricultural University, Zhengzhou, Henan 450046,
- 7 China
- 8 ² Key Laboratory of Farmland Quality Conservation in the Huang-Huai-Hai Plain, Ministry of
- 9 Agriculture and Rural Affairs, Zhengzhou 450046, China;
- 10 3 Key Laboratory of Soil Pollution Prevention, Control and Remediation in Henan Province, Zhengzhou
- 11 450046, China.
- 12 Correspondence to: Hongen Liu, Email: liuhongen7178@126.com; Yupeng Zhang, Email:
- 13 zhangyp@henau.edu.cn
- 14 **Abstract.** Ammonia emissions from agriculture are the primary source of atmospheric reactive nitrogen,
- 15 significantly impacting air pollution, soil acidification, eutrophication of water bodies, and human health.
- 16 Accurate quantification of ammonia from different sources is crucial for effective mitigation. In this
- 17 study, the air extraction method was employed to collect gases from livestock farms, and the δ¹⁵N values
- $18 \qquad \text{of volatilized ammonia (NH$_3$) from the animal husbandry industry in the southern Huang Huai Hai} \\$
- 19 Plain of China were analyzed using stable nitrogen isotopes. The results show that isotopic signatures
- differ significantly among livestock types: dairy cows (-20.6% \pm 0.8%), laying hens (-27.4% \pm 1.0%),
- and pigs ($-38.4\% \pm 1.7\%$). These livestock-derived signatures are distinct from those associated with
- 22 combustion sources (-7.0% \pm 2.1%) and traffic emissions (6.6% \pm 2.1%), and they exhibit considerably
- 23 lower variability than fertilizer-derived signatures. Overall, this work provides high-precision isotopic
- 24 source signatures for livestock operations, offering essential parameters for regional atmospheric
- ammonia source apportionment and highlighting the need for locally tailored mitigation strategies.







27 Graphical Abstract.

26

28

29

30

31

32

33

34

35

36

37

38

39

40

41

42

43

44

45

46 47

1. Introduction

Ammonia (NH₃) is a highly reactive and abundant nitrogenous gas in the atmosphere. It is classified as a major alkaline species and readily reacts with sulfuric acid and nitric acid to produce ammonium sulfate ((NH₄)₂SO₄) and ammonium nitrate (NH₄NO₃) (Kawashima et al., 2023; Kirkby et al., 2011). These compounds can form particulate ammonium salts or interact with organic aerosols to generate secondary aerosols. In moderately polluted environments, the mass fraction of these ammoniumcontaining particles within PM_{2.5} is relatively low (Huang et al., 2014; Yang et al., 2011). Under severe pollution conditions, however, ammonium sulfate, ammonium nitrate, and other ammonium salts can account for up to approximately 50% of the total PM_{2.5} mass (Battye, 2003; Beusen et al., 2008; Goebes et al., 2003). As a key precursor of secondary inorganic aerosols, NH3 is a primary contributor to haze formation and constitutes a substantial component of PM_{2.5} in polluted atmospheres (Wu et al., 2024; Xiang et al., 2022). Excessive ammonia emissions also drive a range of environmental problems, including soil acidification, climate perturbation, reduced atmospheric visibility, and eutrophication of aquatic ecosystems (Huang et al., 2012; Jiang et al., 2021). Consequently, reducing NH₃ emissions has recently been proposed as a strategy to mitigate smog pollution in China (Liu et al., 2019). Over the past few decades, substantial changes in air quality have been observed across many countries worldwide (Boyle, 2017; Warner et al., 2017). Notably, China has consistently ranked first in global ammonia (NH₃) emissions (Liu et al., 2013). Current NH₃ emission inventories identify the principal sources as agricultural activities-including fertilizer application and livestock and poultry farming-and non-agricultural sources, such as combustion processes and vehicular emissions (Bouwman

49

50

51

52

53

54

55 56

57

58

59

60

61

62

63

64

65

66

67

68

69

70

71

72

73

74

75

76

77





et al., 1997; Schlesinger and Hartley, 1992; Streets et al., 2003). It is widely recognized that agriculture represents the predominant source of atmospheric NH₃, contributing over 70% of total emissions (Meng et al., 2017; Xu et al., 2024), accounting for more than 70% of the total (Ma et al., 2021; Ti et al., 2019), with livestock and poultry farming alone accounting for for 50% to 60% of agricultural NH₃ emission (Huang et al., 2012; Wang et al., 2018). Despite this, substantial uncertainty remains regarding the contribution of livestock-derived NH₃ to nitrogen deposition (Elliott et al., 2019), and estimating these contributions using satellite remote sensing and livestock emission inventories remains challenging (Beusen et al., 2008; Li et al., 2023a; Van Damme et al., 2018). These conventional approaches typically rely on fixed emission factors, such as unit animal excretion coefficients, which are limited by temporal lags and insufficient spatial resolution, thereby hindering the capture of real-time variations in NH₃ emissions and the resulting nitrogen deposition at the farm scale. In contrast, nitrogen stable isotope analysis (δ^{15} N) provides a direct and highly effective approach for tracing the sources of NH₃ and NH₄⁺ (Bhattarai et al., 2020; Xiao et al., 2020). This methodology relies on the principle that distinct emission sources and environmental processes generally exhibit unique isotopic fingerprints (Elliott et al., 2019; Li et al., 2024; Sui et al., 2020), defined by the ratio of heavy (15N) to light (14N) nitrogen isotopes in collected samples (Song et al., 2021). Numerous studies have employed stable nitrogen isotope (δ^{15} N) techniques to quantify the contributions of combustion, transportation, and agricultural activities to atmospheric NH3 and NH4+ (Xiang et al., 2022; Xie et al., 2008). For example, during the corn growing season in Northeast China, δ¹⁵N values of NH₃ volatilized from farmland exhibited a wide range, from -38.0% to -0.2%. Notably, δ^{15} N emission rates were considerably lower during the early stages of corn growth compared to later stages, indicating clear seasonal variation (Song et al., 2024). Under different fertilization regimes, significant differences in δ^{15} N-NH₃ emissions were observed, with values fluctuating between -46.0% and -4.7% throughout the volatilization period (Ti et al., 2021). Previous studies report that δ^{15} N-NH₃ and $\delta^{15}\text{N-NH}_4^+$ emissions from combustion sources (-7.6‰ to +16.2‰) predominate in winter, contributing up to 51.6% of total ammonia emissions (Xiao et al., 2022, 2025; Zhou et al., 2021). In contrast, NH₃ emissions from vehicle exhaust exhibit relatively high δ^{15} N values (13.7 ± 3.7%) (Savard et al., 2017; Xi et al., 2023). However, these emissions are primarily localized in urban environments. Currently, limited studies have reported the $\delta^{15}N$ characteristics of ammonia from livestock and poultry farming. Existing data mostly rely on passive sampling methods (Berner and David Felix, 2020;





79 surrounding farms (pig farms: -35.1% to -10.5%; cattle farms: -24.7% to -11.3%). Additional research 80 has quantified δ^{15} N variability in livestock and poultry (-31.0% to -15.0%) through simulated ammonia 81 emissions during manure management processes (Hristov et al., 2009). It is noteworthy that δ^{15} N-NH₃ 82 fluctuations in livestock and poultry operations may also depend on animal growth stages and 83 reproductive status.. 84 The MixSAIR model has primarily been employed to apportion the contributions of atmospheric emission sources using isotope analysis (Chang et al., 2016; Walters et al., 2022). However, there is no 85 86 universally fixed δ^{15} N-NH₄⁺ value for each emission source. As a result, substantial variations in reported 87 $\delta^{15}\text{N-NH}_4^+$ values for the same source have been documented across different studies. To date, no 88 research has validated changes in δ^{15} N-NH₄⁺ resulting specifically from livestock and poultry farm 89 emissions, nor has the relationship between δ^{15} N-NH₄⁺ from different sources and regional variations 90 been examined. To obtain more accurate assessments of δ^{15} N-NH₃ variations associated with ammonia 91 emissions from livestock and poultry farming, and to achieve reliable atmospheric NH₃ source 92 apportionment, it is essential to characterize the correlation between δ^{15} N-NH₄⁺ from different sources 93 and regional differences. In this study, active dynamic sampling methods were used to collect ammonia 94 emissions from intensive pig farms, dairy farms, and laying hen farms located in the southern region of 95 the Huang-Huai-Hai Plain. Meta-analysis techniques were employed to analyze the δ^{15} N signatures of 96 different ammonia emission sources. The specific objectives of this research are: (1) to determine the 97 δ^{15} N-NH₄⁺ values of emissions from livestock and poultry housing at various growth stages; and (2) to 98 investigate the relationship between δ^{15} N-NH₄⁺ from different sources and regional variations.

Chang et al., 2016; Ti et al., 2018), which assess $\delta^{15}N$ changes by collecting wet deposition samples

2. Materials and methods

99

100

101

102

103

104

105

2.1. Sampling points in the study area and sample collection and processing.

The sampling experiment at the farm was conducted from May 9, 2024, to December 6, 2024. No samples were collected in July and August due to the absence of livestock or poultry during these months. The collected samples covered the entire breeding period of fattening pigs and the period from chicks to peak egg production in laying hens. Throughout the trial period, six batches of samples were obtained, amounting to a total of 120 samples for measuring ammonia emissions from livestock and poultry

107

108

109

110

111

112

113

114

115

116

117

118

119

120

121

122

123

124

125

126

127

128

129

130

131

132

133

134

135





as severe, whereas samples collected under clean atmospheric conditions corresponded to air quality classified as excellent. Samples were collected using atmospheric samplers (Beijing Ke'an Labor Protection Company) at a flow rate of 0.1 to 2 L·min⁻¹, with each sample collected over a duration of 60 minutes. The intensive fattening pig farm is located in Luoyang City, Henan Province (112.71° E, 34.52° N), with no other livestock operations in the surrounding area. The sampled fattening pig farm houses 2,600 pigs distributed across four fully enclosed pig houses. One of these houses was selected as the target sampling site. The sampling procedure was as follows: an atmospheric sampler was positioned 2.0 meters from the exhaust vent of the livestock and poultry house at a height of 1.6 meters, corresponding to the central height of the exhaust outlet. T The sampling duration was set to 60 minutes, with the gas flow rate maintained at 2 L·min⁻¹ using a flow meter. A bubbler absorption bottle filled with absorption solution was used to collect NH3. Three atmospheric samplers were operated simultaneously during each sampling event. Figure 1 marks the sampling points of the intensive pig farms with green pentagrams. In the case of intensive laying hens farms, each building houses approximately 15,000 laying hens and is fully enclosed, with a total of 300,000 laying hens being raised. The sampling site is located in Zhengzhou City, Henan Province (114.03° E, 34.59° N). One building was selected as the target sampling point, with the sampling method mirroring that used for the fattening pig farms. As shown in Figure 1, the light blue pentagons represent the sampling points of intensive layer farms. The intensive dairy farm operates with an open-style barn design, housing 400 dairy cows per barn, with a total of 4,000 dairy cows being raised. Four atmospheric samplers were installed in the passageways of the dairy barns, with each sampler spaced 10 meters apart and positioned at a height of 1.6 meters. The dairy farm is located in Zhengzhou City, Henan Province (114.11° E, 34.81° N). The sampling time and method remained consistent with those described above. In Figure 1, the dark blue pentagons represent the sampling points of intensive dairy farms. To investigate the variations in δ^{15} N levels associated with differing degrees of air pollution, samples collected for $\delta^{15}N$ measurement during periods of severe smog and when air quality was pristine. The sampling location was situated on a spacious lawn within the campus of Henan Agricultural University, devoid of tall buildings or traffic. The sampling point is illustrated in Figure 1, where the pink triangle represents the sampling site for both haze and clean air (Longitude 113.82° E, Latitude 34.80° N). Each

housing. On days when samples were collected during hazy weather, the air pollution level was classified

150

151

152

153

154

155

156157

158





- sampling event utilized three atmospheric samplers, positioned at a height of 1.6 meters, with the duration
 of sampling aligned with that of the livestock farm.
- The collected sample solution is transferred into a centrifuge tube and returned to the laboratory,
 where the concentration of NH₃ is measured using a UV spectrophotometer. The detection method
 adheres to the guidelines outlined in "Determination of Ammonia Nitrogen in Water by Salicylic Acid
 Spectrophotometry" (HJ 536-2009), and the calculation method is presented in Equation (1):

$$\rho_N = \frac{A_s - A_b - a}{b \times V} \times D \tag{1}$$

- 143 Where, ρ_N represents the mass concentration of ammonia nitrogen in the water sample (expressed as N), 144 in mg·L⁻³. The variables are defined as follows: A_s denotes the absorbance of the sample, while A_b 145 indicates the absorbance of the blank experiment, which is prepared from the same batch as the sample. 146 The parameters a and b correspond to the intercept and slope of the calibration curve, respectively. 147 Additionally, V refers to the volume of the water sample taken, measured in mL, and D signifies the 148 dilution factor of the water sample.
 - The analytical method described employs the bromate-hydroxylamine chemical approach (Soler-Jofra et al., 2016; Zhang et al., 2007). Initially, a potassium bromate-potassium bromide solution reacts under acidic conditions to produce bromine, which subsequently reacts in a strongly alkaline environment to generate bromate, a potent oxidizing agent capable of oxidizing NH₄⁺ to NO₂⁻. In the following step, hydroxylamine hydrochloride reduces NO₂⁻ in an acidic environment to form N₂O. The resultant N₂O is then analyzed using a stable isotope ratio mass spectrometer, along with a multi-purpose online gas preparation device, and an automatic sampler, to determine the δ^{15} N value. For each sample analysis, four international standard materials for NH₄⁺ (IAEA-N-1, USGS-25, IAEA-N-2, and USGS-26, with δ^{15} N concentrations of 0.4‰, -30.41‰, 20.3‰, and 53.75‰, respectively) are processed simultaneously.



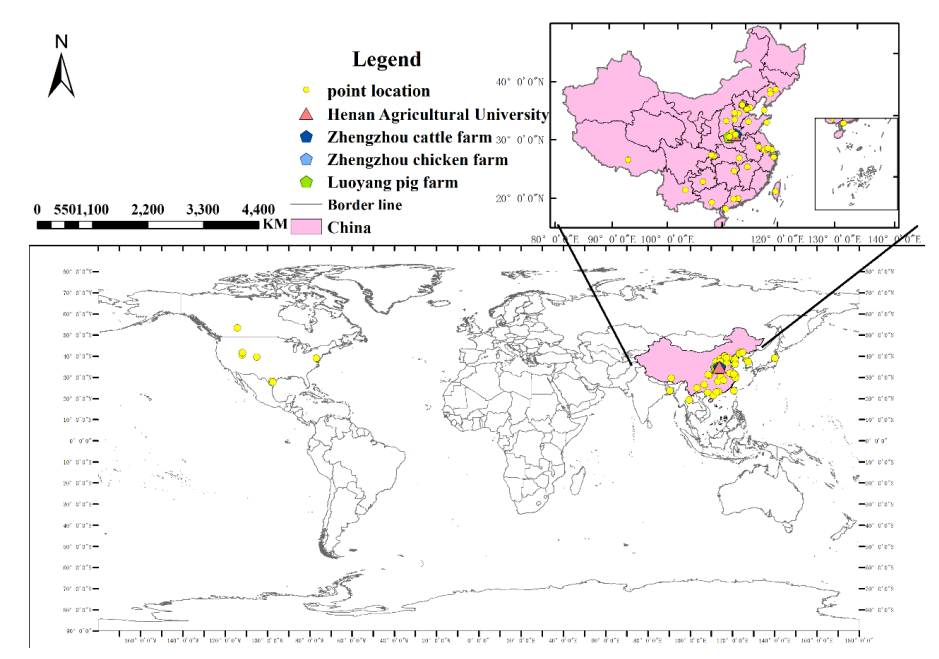


Figure 1. Sampling sites of livestock farms, haze weather, and clear weather in this study, extracted from the main research sampling locations. Yellow dots represent the main global research sampling sites, pink triangles represent sampling sites during haze and clear weather, dark blue pentagons represent cattle farms, light blue pentagons represent layer farms, and green pentagons represent fattening pig farms.

2.2. Data collection and processing

We screened articles published between January 2000 and January 2025 regarding the sources of $\delta^{15}\text{N-NH}_3$ and $\delta^{15}\text{N-NH}_4^+$. Specifically, we utilized ISI Web of Science, Google Scholar, and PubMed, employing the search terms " $\delta^{15}\text{N}$," "NH₃," "ammonia emissions," and "isotopes" to identify relevant literature. Studies included in our analysis were required to meet the following criteria: (1) Samples must be measured for either $\delta^{15}\text{N-NH}_3$ or $\delta^{15}\text{N-NH}_4^+$; (2) Experiments must encompass at least one of the following: combustion, fertilization, agriculture, transportation, or livestock farming; (3) The number of experimental replicates and sampling events must be explicitly reported; (4) Samples must primarily consist of atmospheric NH₃ or PM_{2.5}, and detection must employ chemical methods. A total of 37 documents were included in the analysis. This dataset comprehensively encompasses multiple meta-analyses and original studies, detailing changes in $\delta^{15}\text{N-NH}_3$ and $\delta^{15}\text{N-NH}_4^+$ from combustion sources, transportation sources, agricultural sources, and livestock farming sources; the proportion of $\delta^{15}\text{N}$ values

177

178

179

182

183

184

185186

187

188

189

190

191

192

193

194

195

196197

198

199

200

201

202





in the atmosphere; geographical location (latitude and longitude); and the GDP of each city where samples were collected. If the data in the literature was presented solely in chart form, we utilized WebPlotDigitizer-4.7 (https://apps.automeris.io/wpd4/) to extract the data. We categorized the collected data into five distinct groups: combustion, transportation, farmland, livestock farming, and PM_{2.5}.

A total of 126 samples were collected, and 41 literature references were gathered. Data analysis was performed using Excel, SPSS, and Python version 3.11.

3. Result and discussion

3.1. Temporal Variations in Ammonia Emissions and $\delta^{15}N$ Signatures from Livestock Farms

During the sampling period from May to December, ammonia emissions varied significantly among the three farm types: 4.9 to 6.7 mg·m⁻³ for fattening pigs (Figure 2a), 1.7 and 2.5 mg·m⁻³ for dairy cows (Figure 2b), and 3.8 to 7.1 mg·m⁻³ for laying hens (Figure 2c), with the latter exhibiting substantial temporal fluctuations. NH₃ emissions from fattening pigs peaked when the pigs reached 130 kg·head⁻¹ (Figure 2a), For laying hens, NH3 concentrations initially increased and subsequently declined in response to temperature variations, reflecting enhanced urease activity within the housing environment, which accelerates urea hydrolysis and promotes NH₃ volatilization.δ¹⁵N-NH₄⁺ levels at the livestock farms showed significant temporal variation (p < 0.05) (Groot Koerkamp et al., 1998; Rosa et al., 2020). From May to June, the δ^{15} N-NH₄⁺ From May to June, δ 15N-NH4+ increased from -31.0% to -25.2% in fattening pig farms and from -26.4% to -24.6% in laying hen farms. In September, δ^{15} N-NH₄+ values from fattening pig farms $(-13.3 \pm 1.3\%)$ were significantly higher than those from laying hen and dairy cow farms (-13.9 \pm 0.9%), which were comparable. Over the following three months, δ^{15} N-NH₄⁺ levels decreased significantly across both farm types. As illustrated in Figure 2, the highest NH₃ concentration at the dairy farm $(2.5 \pm 0.3 \text{ mg} \cdot \text{m}^{-3})$ occurred in October, coinciding with the lowest $\delta^{15}\text{N-NH}_4^+$ values. while laying hen farms also recorded minimum δ¹⁵N-NH₄+ during this period of elevated NH₃. Conversely, the lowest δ¹⁵N-NH₄⁺ at fattening pig farms was observed in December, despite peak NH₃ concentrations. NH₃ concentrations differed significantly between hazy and clear weather in December (Figure 2d), with δ^{15} N-NH₄⁺ values being significantly higher under clear conditions (1.9 \pm 0.8‰) than under hazy conditions (1.6 \pm 0.2%; p < 0.05).





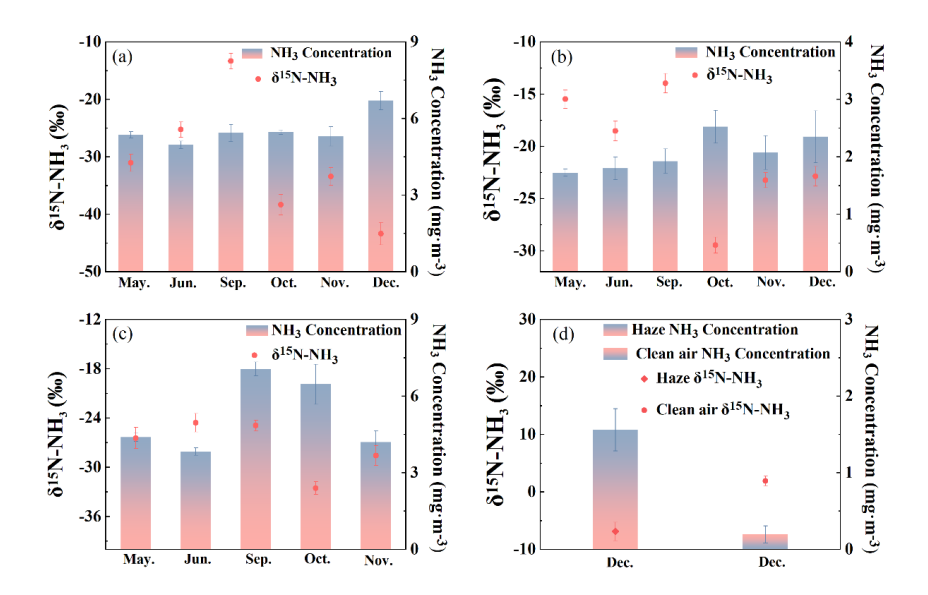
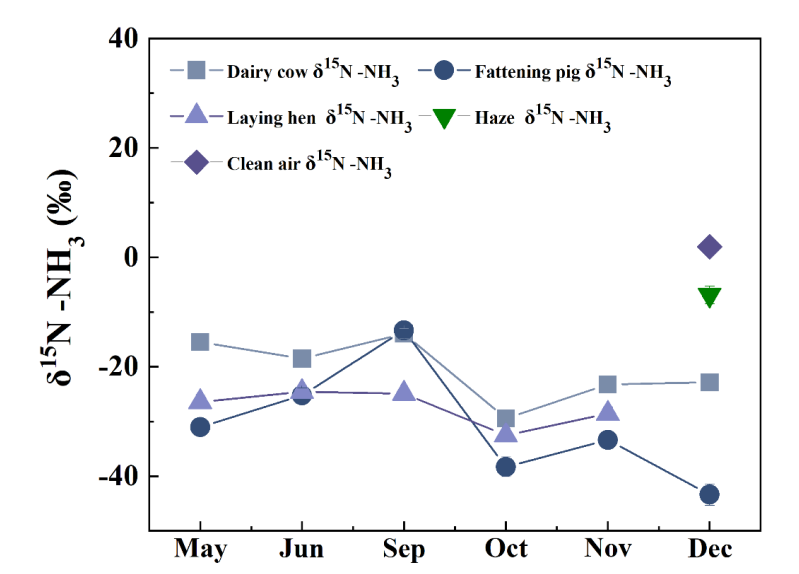


Figure 2. Changes in NH₃ emissions and δ^{15} N-NH₄⁺ values outside the livestock farms among different months. (a)Fatting pig farm; (b)Dairy cow farm; (c) Laying hens farm; (d) Comparison of Haze and clean air samples. Statistical difference was calculated by T-test, P < 0.05, n = 3.

As illustrated in Figure 3, throughout the entire monitoring period, ammonia (NH₃) sources form the farms exhibited nitrogen depletion, indicated by negative $\delta^{15}\text{N-NH}_4^+$ values. Overall, $\delta^{15}\text{N-NH}_4^+$ values exhibited significant fluctuations in dairy and fattening pig farms, while variations were comparatively moderate in laying hens farms. Notably, the $\delta^{15}\text{N-NH}_4^+$ values at dairy cattle farms displayed substantially greater overall changes during the monitoring period compared to those in laying hens and fattening pig farms. The arithmetic mean value at fattening pig farms was -30.8 \pm 1.6‰, the lowest among the three types of farms, whereas the $\delta^{15}\text{N-NH}_4^+$ values in laying hens manure remained at an intermediate level throughout the entire period. From October to December, the $\delta^{15}\text{N-NH}_4^+$ values at livestock and poultry farms were generally lower than those observed in the first half of the monitoring period (Figure 3). However, when comparing hazy and clear weather conditions, the $\delta^{15}\text{N-NH}_4^+$ values for all three types of farms consistently remained at a relatively low level during this timeframe (Figure 3).





221

222

223

224

225

226

227

228

229

230

231

232

233

234

Figure 3. Changes of δ^{15} N-NH₄⁺ abandance at intensive livestock farms during the sampling period. Hazy and clean air were also sampled at December. The air sample of laying hens in December was missed, because of death of chicken by avian influenza.

3.2. Comparison with Literature and Implications for Local Sources

During the monitoring period, the δ^{15} N-NH₄⁺ values ranged from -50.0% to -10.0% (Figure 4a). For fattening pigs, δ^{15} N-NH₄⁺ values averaged -38.4% \pm 1.8% between October and December, which was significantly lower than the previously reported range of -27.10% to -31.7% (Chang et al., 2016) Notably, the overall variation remained within the δ^{15} N-NH₄⁺ emission ranges report for fattening pigs in other studies (Bhattarai and Wang, 2023; Wang et al., 2022). Furthermore, due to differences in livestock management practices and nitrogen content in feed, the $\delta^{15}\text{N-NH}_4^+$ values from dairy farms in this study, averaging -29.4% ± 13.9%, were substantially lower than those reported by Martine M et al. $(20.5\% \pm 34.5\%)$ (Savard et al., 2017). Comparison with δ^{15} N-NH₄⁺ values measured in dairy farms in Akita, Japan, were -22.5% \pm -14.6% (Kawashima, 2019), no significant difference was observed relative to the values obtained in this study. https://doi.org/10.5194/egusphere-2025-4460 Preprint. Discussion started: 18 November 2025 © Author(s) 2025. CC BY 4.0 License.

235

236

237

238

239

240

241

242

243

244245

246

247248

249

250

251

252

253

254





37.9% to -22.9% based on passive sampling techniques. Previous research has shown that active sampling generally yields higher δ^{15} N values than passive sampling (Kawashima and Ono, 2019; Pan et al., 2020). This discrepancy arises from the diffusion-driven nature of passive samplers, in which lighter NH₃ molecules are preferentially adsorbed. Consequently, passive sampling typically produces δ^{15} N values that deviate by approximately 15% from those obtained by active sampling (Bhattarai and Wang, 2023; Skinner et al., 2006). Variations in δ^{15} N-NH₄⁺ values are known to occur among different livestock species. During the monitoring period, $\delta^{15}N-NH_4^+$ values from laying hen farms were consistently lower than those from dairy farms but higher than those from fattening pig farms, consistent with previously reported trends. This pattern suggests that δ^{15} N-NH₄⁺ variations in emitted NH₃ are not primarily driven by animal body weight but are instead strongly modulated by environmental conditions (Choi et al., 2017; Qu and Zhang, 2021). In agreement with earlier studies, δ¹⁵N-NH₄+ emissions from fattening pig and laying hen farms differed significantly from previously documented values, whereas no significant difference was observed for dairy cattle farms. Furthermore, the magnitude of $\delta^{15}N-NH_4^+$ fluctuations across the three farm types was smaller than that reported in earlier literature. Comparison with major atmospheric NH₃ sources further demonstrated that the δ^{15} N-NH₄ values measured in this study diverged substantially from those associated with combustion (-7.0% \pm 2.1%), fertilization application (-38.0%) \pm 0.2‰), and transportation (6.6‰ \pm 2.1‰). Based on δ^{15} N-NH₄⁺ signatures measured under both hazy and clear weather conditions, it can therefore be inferred that agricultural and livestock emissions are not the dominant contributors to atmospheric NH3 in Zhengzhou. Instead, traffic exhaust and combustion sources appear to constitute the primary contributors.



257

258

259

260

261

262

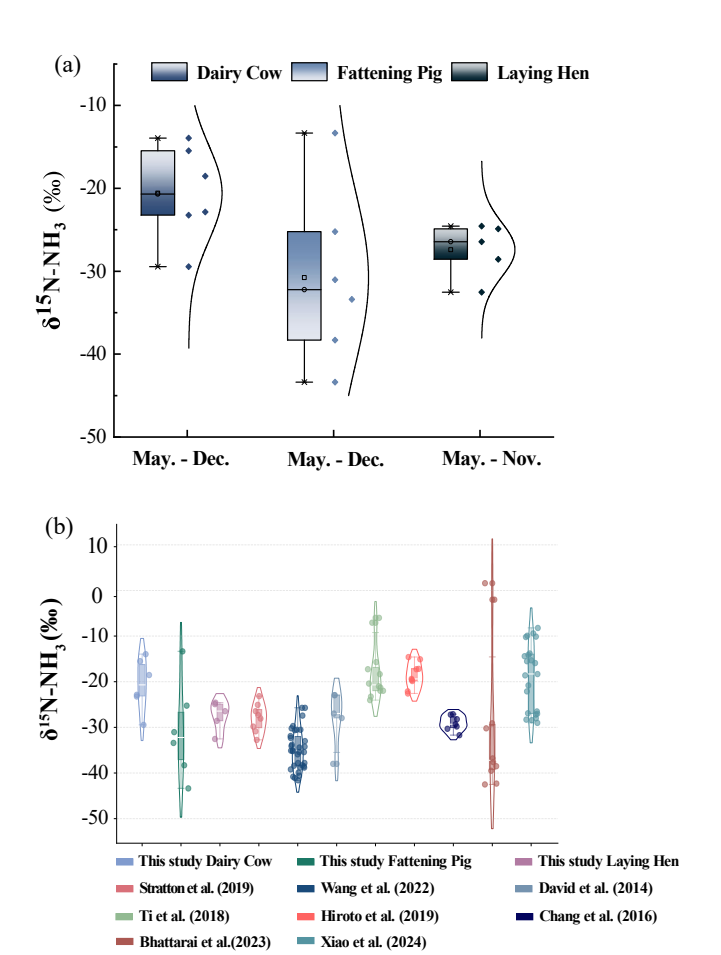


Figure 4. Comparison of $\delta^{15}N$ -NH₄⁺ values within different livestock farms and historical reported data. (a)Comparison of the $\delta^{15}N$ -NH₄⁺ values among different livestock farms; (b)Comparison of the $\delta^{15}N$ -NH₄⁺ values from present study with previously reported data.

$\textbf{3.3. Global Variability of NH}_{\textbf{3}} \, \textbf{Source Signatures and Challenges for Source Apportionment}$

Ammonia emissions that contribute to urban smog primarily arise from combustion activities, vehicle exhaust, agriculture fertilization, and livestock production. As national economies expand, the frequency and severity of smog events have intensified. Figure 5a (slope: 0.026, intercept: 1.6323, R²:

264

265

266

267

268

269

270

271

272

273

274

275

276

277

278

279

280

281

282

283

284

285

286 287





0.0963) shows that from 2000 to 2025, when GDP remains below 70 billion USD, atmospheric δ^{15} N-NH₄⁺ signatures predominantly reflect fertilizer-derived emissions from agricultural regions and NH₃ volatilization from livestock operations (Kawashima et al., 2022; Kawashima and Kurahashi, 2011). This pattern indicates that lower-income regions rely heavily on agriculture and animal husbandry as the foundational components of their economies (Leng et al., 2018).

When GDP increases to between 80 billion and 300 billion USD, the contribution of combustionrelated and vehicular sources to δ¹⁵N-NH₄⁺ becomes increasingly prominent. Notably, vehicle exhaust remains the dominant contributor within this GDP interval, suggesting that transportation serves as a key economic driver during mid-stage development. In densely populated and economically advanced cities, rapid vehicle growth further amplifies the influence of transportation-related δ^{15} N-NH₄⁺ signatures(Lim et al., 2022; Pan et al., 2018; Stratton et al., 2019). Throughout the entire dataset, vehicle exhaust and combustion together account for nearly 70% of ammonia emissions(Wu et al., 2019). Once GDP surpasses 300 billion USD, δ^{15} N-NH₄⁺ from combustion becomes the dominant atmospheric source, while the relative contribution from vehicle exhaust begins to decline and emissions from agricultural fertilization and livestock farming become negligible (Li et al., 2023b). It is important to note that sampling sites in the present study were located near power plants (Lim et al., 2019; Zou et al., 2022), whereas comparison data from previous studies were collected in urban cores. This spatial difference further supports the conclusion that in highly developed cities, shifts in economic structure lead to combustion sources emerging as the principal contributors to atmospheric NH3 under both hazy and clear meteorological conditions. As illustrated in Figure 5b, the proportion of $\delta^{15}N-NH_4^+$ attributed to combustion and vehicular sources has increased over time. This temporal trend suggests that, with economic growth, agricultural and livestock emissions no longer represent the dominant contributors to atmospheric ammonia.

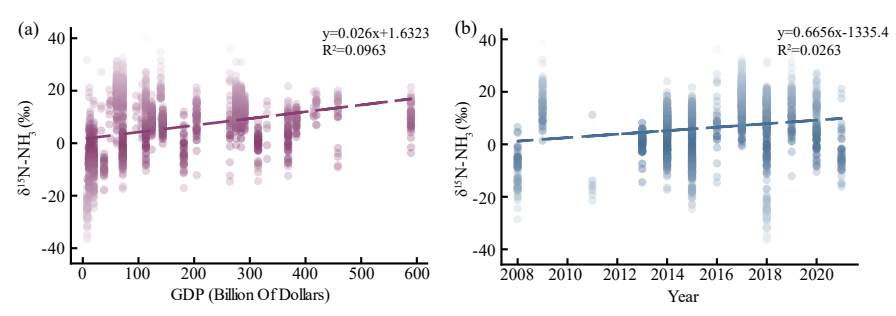


Figure 5. Changes of δ¹⁵N-NH₄⁺ values among different GDP cities and years. (a) The relationship





between GDP and $\delta^{15}N-NH_4^+$ values; (b) Changes of $\delta^{15}N-NH_4^+$ values reported between 2008 to 2021.

The extracted dataset was classified into four major emission categories-livestock farming, combustion, farmland fertilization, and vehicle exhaust-and subsequently subjected to statistical evaluation. As illustrated in Figure 6, δ^{15} N-NH₄+ values associated with combustion sources showed strong consistency with previously reported ranges (Chang et al., 2021). Although traffic exhaust and livestock-related δ^{15} N-NH₄+ values exhibited moderate dispersion, both sources remained within relatively well-defined isotopic ranges. In sharp contrast, δ^{15} N-NH₄+ signatures following farmland fertilization displayed pronounced heterogeneity, covering nearly the entire isotopic spectrum reported for combustion, livestock, and vehicular emissions. This extensive variability highlights substantial regional differences in agricultural ammonia emission processes (Felix et al., 2014; Li et al., 2023b). Consequently, accurate source apportionment of atmospheric NH₃ requires distinguishing dominant local emission pathways rather than relying solely on generalized isotopic patterns (Chen et al., 2022; Zhang et al., 2023).

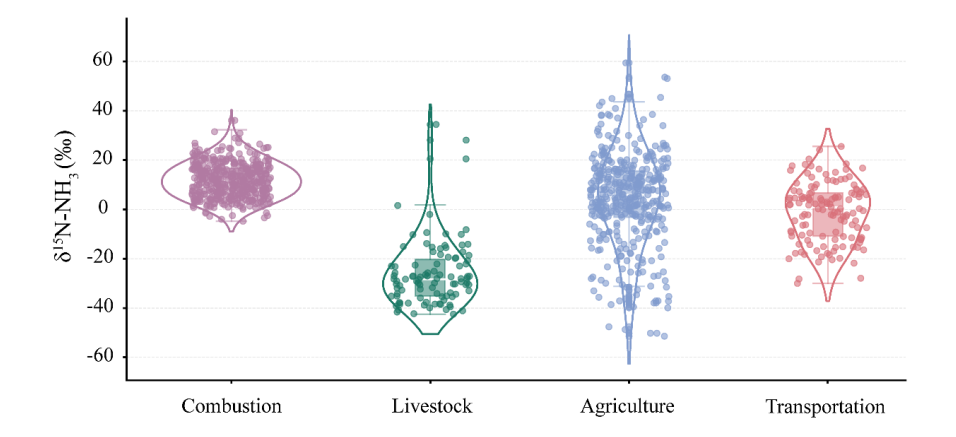


Figure 6. Statistical analysis of extracted data categorized by source: combustion sources, livestock and poultry farming sources, agricultural sources, and transportation exhaust sources.

4. Summary

This study establishes high-precision $\delta^{15}N$ signatures for ammonia emissions from three dominant intensive livestock systems in the Huang-Huai-Hai Plain. Distinct isotopic fingerprints were identified

308

309

310

311

312

313

314315

316

317

318

319

320





for dairy operations (-20.6‰ \pm 0.8‰), laying hen facilities (-27.4‰ \pm 1.0‰), and fattening pig farms (-38.4‰ \pm 1.7‰), underscoring clear differences among livestock categories. Our results further demonstrate that isotopic signatures vary dynamically with NH₃ volatilization intensity, highlighting the need to incorporate volatilization-driven fractionation effects into isotope-based source apportionment frameworks. When compared with ambient δ^{15} N-NH₄⁺ measurements in Zhengzhou, the newly constrained source end-members indicate that non-agricultural sources-particularly vehicular emissions and combustion-are likely major contributors to urban atmospheric ammonia. This interpretation, however, requires validation through comprehensive isotopic mixing and dispersion modeling. Moreover, global-scale evaluation reveals that the exceptional variability of δ^{15} N associated with fertilized soils continues to pose a substantial challenge for accurate identification of agricultural contributions. Collectively, the findings presented here provide critical isotopic constraints that can enhance regional atmospheric chemistry models and support the design of more precise and effective ammonia emission control policies.

Author Contributions

- 321 J.W. Drafting, Formal Analysis, Data Management, Methodology, Investigation; Z.N. Formal Analysis,
- 322 Data Management, Methodology, Investigation; Y.Z. Conceptualization, Data Management,
- 323 Visualization, Funding Acquisition, Drafting, Formal Analysis, Writing Review & Editing; X.J. Data
- 324 Management, Visualization; H.L. Data Management, Methodology; P.Z. Formal Analysis, Data
- 325 Management; H.L. Writing Review & Editing, Funding Acquisition, Conceptualization, Supervision.

326 Competing interest

- 327 The authors declare that they have no known competing financial interests or personal relationships that
- 328 could have influenced the work reported in this paper.
- 329 Acknowledgments. This research was supported by the National Key Research and Development
- 330 Program of China (2021 YFD 1700900), the Industrial Technology System for Cultivated Land
- 331 Protection in Henan Province (HARS-22-19-S), the Natural Science Foundation of Henan Province
- 332 (Grant No. 252300420043), and the Key Research and Development Program of Henan Province (Grant
- 333 No. 251111112200).

Data availability

334





- 335 All data are available in the text, Supplement or publicly on Zenodo (DOI 10.5281/zenodo.17639507).
- 336 **References:**
- 337 Battye, W.: Evaluation and improvement of ammonia emissions inventories, Atmos. Environ., 37, 3873-
- 338 3883, https://doi.org/10.1016/S1352-2310(03)00343-1, 2003.
- 339 Berner, A. H. and David Felix, J.: Investigating ammonia emissions in a coastal urban airshed using
- 340 stable isotope techniques, Sci. Total Environ., 707, 134952,
- 341 https://doi.org/10.1016/j.scitotenv.2019.134952, 2020.
- 342 Beusen, A. H. W., Bouwman, A. F., Heuberger, P. S. C., Van Drecht, G., and Van Der Hoek, K. W.:
- 343 Bottom-up uncertainty estimates of global ammonia emissions from global agricultural production
- 344 systems, Atmos. Environ., 42, 6067–6077, https://doi.org/10.1016/j.atmosenv.2008.03.044, 2008.
- 345 Bhattarai, N. and Wang, S.: Active vs. passive isotopic analysis: insights from urban beijing field
- 346 measurements and ammonia source signatures, Atmos. Environ., 314,
- 347 https://doi.org/10.1016/j.atmosenv.2023.120079, 2023.
- 348 Bhattarai, N., Wang, S., Xu, Q., Dong, Z., Chang, X., Jiang, Y., and Zheng, H.: Sources of gaseous NH₃
- 349 in urban beijing from parallel sampling of NH₃ and NH₄⁺, their nitrogen isotope measurement and
- 350 modeling, Sci. Total Environ., 747, 141361, https://doi.org/10.1016/j.scitotenv.2020.141361, 2020.
- 351 Bouwman, A. F., Lee, D. S., Asman, W. a. H., Dentener, F. J., Van Der Hoek, K. W., and Olivier, J. G. J.:
- 352 A global high-resolution emission inventory for ammonia, Glob. Biogeochem. Cycles, 11, 561-587,
- 353 https://doi.org/10.1029/97GB02266, 1997.
- 354 Boyle, E.: Nitrogen pollution knows no bounds, Science, 356, 700-701,
- 355 https://doi.org/10.1126/science.aan3242, 2017.
- 356 Chang, Y., Liu, X., Deng, C., Dore, A. J., and Zhuang, G.: Source apportionment of atmospheric ammonia
- 357 before, during, and after the 2014 APEC summit in beijing using stable nitrogen isotope signatures,
- 358 Atmospheric Chem. Phys., 16, 11635–11647, https://doi.org/10.5194/acp-16-11635-2016, 2016.
- Chang, Y., Zhang, Y.-L., Kawichai, S., Wang, Q., Van Damme, M., Clarisse, L., Prapamontol, T., and
- 360 Lehmann, M. F.: Convergent evidence for the pervasive but limited contribution of biomass burning to
- 361 atmospheric ammonia in peninsular southeast Asia, Atmospheric Chem. Phys., 21, 7187-7198,
- 362 https://doi.org/10.5194/acp-21-7187-2021, 2021.
- 363 Chen, T.-Y., Chen, C.-L., Chen, Y.-C., Chou, C. C.-K., Ren, H., and Hung, H.-M.: Source apportionment
- and evolution of N-containing aerosols at a rural cloud forest in taiwan by isotope analysis, Atmospheric
- $365 \qquad \text{Chem. Phys., } 22, 13001-13012, \\ \text{https://doi.org/} 10.5194/acp-22-13001-2022, 2022. \\$
- 366 Choi, W.-J., Kwak, J.-H., Lim, S.-S., Park, H.-J., Chang, S. X., Lee, S.-M., Arshad, M. A., Yun, S.-I., and
- 367 Kim, H.-Y.: Synthetic fertilizer and livestock manure differently affect δ15N in the agricultural landscape:
- 368 a review, Agric. Ecosyst. Environ., 237, 1–15, https://doi.org/10.1016/j.agee.2016.12.020, 2017.





- 369 Elliott, E. M., Yu, Z., Cole, A. S., and Coughlin, J. G.: Isotopic advances in understanding reactive
- 370 nitrogen deposition and atmospheric processing, Sci. Total Environ., 662, 393-403,
- 371 https://doi.org/10.1016/j.scitotenv.2018.12.177, 2019.
- 372 Felix, J. D., Elliott, E. M., Gish, T., Maghirang, R., Cambal, L., and Clougherty, J.: Examining the
- 373 transport of ammonia emissions across landscapes using nitrogen isotope ratios, Atmos. Environ., 95,
- 374 563–570, https://doi.org/10.1016/j.atmosenv.2014.06.061, 2014.
- 375 Goebes, M. D., Strader, R., and Davidson, C.: An ammonia emission inventory for fertilizer application
- 376 in the United States, Atmos. Environ., 37, 2539-2550, https://doi.org/10.1016/S1352-2310(03)00129-8,
- 377 2003.
- 378 Groot Koerkamp, P. W. G., Metz, J. H. M., Uenk, G. H., Phillips, V. R., Holden, M. R., Sneath, R. W.,
- 379 Short, J. L., White, R. P. P., Hartung, J., Seedorf, J., Schröder, M., Linkert, K. H., Pedersen, S., Takai, H.,
- 380 Johnsen, J. O., and Wathes, C. M.: Concentrations and emissions of ammonia in livestock buildings in
- 381 northern Europe, J. Agric. Eng. Res., 70, 79–95, https://doi.org/10.1006/jaer.1998.0275, 1998.
- 382 Hristov, A. N., Zaman, S., Vander Pol, M., Ndegwa, P., Campbell, L., and Silva, S.: Nitrogen losses from
- dairy manure estimated through nitrogen mass balance and chemical markers, J. Environ. Qual., 38,
- 384 2438–2448, https://doi.org/10.2134/jeq2009.0057, 2009.
- 385 Huang, R.-J., Zhang, Y., Bozzetti, C., Ho, K.-F., Cao, J.-J., Han, Y., Daellenbach, K. R., Slowik, J. G.,
- 386 Platt, S. M., Canonaco, F., Zotter, P., Wolf, R., Pieber, S. M., Bruns, E. A., Crippa, M., Ciarelli, G.,
- 387 Piazzalunga, A., Schwikowski, M., Abbaszade, G., Schnelle-Kreis, J., Zimmermann, R., An, Z., Szidat,
- 388 S., Baltensperger, U., Haddad, I. E., and Prévôt, A. S. H.: High secondary aerosol contribution to
- 389 particulate pollution during haze events in China, Nature, 514, 218-222,
- 390 https://doi.org/10.1038/nature13774, 2014.
- 391 Huang, X., Song, Y., Li, M., Li, J., Huo, Q., Cai, X., Zhu, T., Hu, M., and Zhang, H.: A high-resolution
- 392 ammonia emission inventory in China, Glob. Biogeochem. Cycles, 26
- 393 https://doi.org/10.1029/2011GB004161, 2012.
- 394 Jiang, H., Zhang, Q., Liu, W., Zhang, J., Pan, K., Zhao, T., and Xu, Z.: Isotopic compositions reveal the
- driving forces of high nitrate level in an urban river: implications for pollution control, J. Clean. Prod.,
- 396 298, 126693, https://doi.org/10.1016/j.jclepro.2021.126693, 2021.
- 397 Kawashima, H.: Seasonal trends of the stable nitrogen isotope ratio in particulate nitrogen compounds
- 398 and their gaseous precursors in akita, japan, Tellus Ser. B-Chem. Phys. Meteorol., 71,
- 399 https://doi.org/10.1080/16000889.2019.1627846, 2019.
- 400 Kawashima, H. and Kurahashi, T.: Inorganic ion and nitrogen isotopic compositions of atmospheric
- 401 aerosols at yurihonjo, Atmos. Environ., 45, 6309–6316, https://doi.org/10.1016/j.atmosenv.2011.08.057,
- 402 2011.
- 403 Kawashima, H. and Ono, S.: Nitrogen isotope fractionation from ammonia gas to ammonium in
- 404 particulate ammonium chloride, Environ. Sci. Technol., 53, 10629-10635,
- 405 https://doi.org/10.1021/acs.est.9b01569, 2019.





- 406 Kawashima, H., Yoshida, O., Joy, K. S., Raju, R. A., Islam, K. N., Jeba, F., and Salam, A.: Sources
- 407 identification of ammonium in PM2.5 duringmonsoon season in Dhaka, bangladesh, Sci. Total Environ.,
- 408 838, https://doi.org/10.1016/j.scitotenv.2022.156433, 2022.
- 409 Kawashima, H., Yoshida, O., and Suto, N.: Long-term source apportionment of ammonium in PM_{2.5} at a
- 410 suburban and a rural site using stable nitrogen isotopes, Environ. Sci. Technol., 57, 1268-1277,
- 411 https://doi.org/10.1021/acs.est.2c06311, 2023.
- 412 Kirkby, J., Curtius, J., Almeida, J., Dunne, E., Duplissy, J., Ehrhart, S., Franchin, A., Gagné, S., Ickes,
- 413 L., Kürten, A., Kupc, A., Metzger, A., Riccobono, F., Rondo, L., Schobesberger, S., Tsagkogeorgas, G.,
- 414 Wimmer, D., Amorim, A., Bianchi, F., Breitenlechner, M., David, A., Dommen, J., Downard, A., Ehn,
- 415 M., Flagan, R. C., Haider, S., Hansel, A., Hauser, D., Jud, W., Junninen, H., Kreissl, F., Kvashin, A.,
- Laaksonen, A., Lehtipalo, K., Lima, J., Lovejoy, E. R., Makhmutov, V., Mathot, S., Mikkilä, J.,
- 417 Minginette, P., Mogo, S., Nieminen, T., Onnela, A., Pereira, P., Petäjä, T., Schnitzhofer, R., Seinfeld, J.
- 418 H., Sipilä, M., Stozhkov, Y., Stratmann, F., Tomé, A., Vanhanen, J., Viisanen, Y., Vrtala, A., Wagner, P.
- 419 E., Walther, H., Weingartner, E., Wex, H., Winkler, P. M., Carslaw, K. S., Worsnop, D. R., Baltensperger,
- 420 U., and Kulmala, M.: Role of sulphuric acid, ammonia and galactic cosmic rays in atmospheric aerosol
- 421 nucleation, Nature, 476, 429–433, https://doi.org/10.1038/nature10343, 2011.
- 422 Leng, Q., Cui, J., Zhou, F., Du, K., Zhang, L., Fu, C., Liu, Y., Wang, H., Shi, G., Gao, M., Yang, F., and
- 423 He, D.: Wet-only deposition of atmospheric inorganic nitrogen and associated isotopic characteristics in
- 424 a typical mountain area, southwestern china, Sci. Total Environ., 616, 55-63,
- 425 https://doi.org/10.1016/j.scitotenv.2017.10.240, 2018.
- 426 Li, K., Xu, D., Zhang, L., Liu, W., Zhan, M., Su, Y., Wu, D., and Xie, B.: Integrated isotopic labeling
- 427 analysis unveils precise proportions of ammonia emissions during composting, J. Clean. Prod., 450,
- 428 141799, https://doi.org/10.1016/j.jclepro.2024.141799, 2024.
- Li, T., Wang, C., Ji, W., Wang, Z., Shen, W., Feng, Y., and Zhou, M.: Cutting-edge ammonia emissions
- 430 monitoring technology for sustainable livestock and poultry breeding: a comprehensive review of the
- 431 state of the art, J. Clean. Prod., 428, 139387, https://doi.org/10.1016/j.jclepro.2023.139387, 2023a.
- 432 Li, T., Li, J., Sun, Z., Jiang, H., Tian, C., and Zhang, G.: High contribution of anthropogenic combustion
- 433 sources to atmosphericinorganic reactive nitrogen in south China evidenced by isotopes, Atmospheric
- 434 Chem. Phys., 23, 6395–6407, https://doi.org/10.5194/acp-23-6395-2023, 2023b.
- Lim, S., Lee, M., Czimczik, C. I., Joo, T., Holden, S., Mouteva, G., Santos, G. M., Xu, X., Walker, J.,
- 436 Kim, S., Kim, H. S., Kim, S., and Lee, S.: Source signatures from combined isotopic analyses of PM2.5
- 437 carbonaceous and nitrogen aerosols at the peri-urban taehwa research forest, south korea in summer and
- 438 fall, Sci. Total Environ., 655, 1505–1514, https://doi.org/10.1016/j.scitotenv.2018.11.157, 2019.
- Lim, S., Hwang, J., Lee, M., Czimczik, C., I., Xu, X., and Savarino, J.: Robust evidence of 14C, 13C,
- and 15N analyses indicating fossil fuel sources for total carbon and ammonium in fine aerosols in Seoul
- 441 megacity, Environ. Sci. Technol., 56, 6894–6904, https://doi.org/10.1021/acs.est.1c03903, 2022.
- 442 Liu, M., Huang, X., Song, Y., Tang, J., Cao, J., Zhang, X., Zhang, Q., Wang, S., Xu, T., Kang, L., Cai,





- 443 X., Zhang, H., Yang, F., Wang, H., Yu, J. Z., Lau, A. K. H., He, L., Huang, X., Duan, L., Ding, A., Xue,
- 444 L., Gao, J., Liu, B., and Zhu, T.: Ammonia emission control in China would mitigate haze pollution and
- 445 nitrogen deposition, but worsen acid rain, Proc. Natl. Acad. Sci., 116, 7760-7765,
- 446 https://doi.org/10.1073/pnas.1814880116, 2019.
- 447 Liu, X., Zhang, Y., Han, W., Tang, A., Shen, J., Cui, Z., Vitousek, P., Erisman, J. W., Goulding, K.,
- 448 Christie, P., Fangmeier, A., and Zhang, F.: Enhanced nitrogen deposition over china, Nature, 494, 459–
- 449 462, https://doi.org/10.1038/nature11917, 2013.
- 450 Ma, R., Zou, J., Han, Z., Yu, K., Wu, S., Li, Z., Liu, S., Niu, S., Horwath, W. R., and Zhu-Barker, X.:
- 451 Global soil-derived ammonia emissions from agricultural nitrogen fertilizer application: a refinement
- 452 based on regional and crop-specific emission factors, Glob. Change Biol., 27, 855-867,
- 453 https://doi.org/10.1111/gcb.15437, 2021.
- 454 Meng, W., Zhong, Q., Yun, X., Zhu, X., Huang, T., Shen, H., Chen, Y., Chen, H., Zhou, F., Liu, J., Wang,
- 455 X., Zeng, E. Y., and Tao, S.: Improvement of a global high-resolution ammonia emission inventory for
- 456 combustion and industrial sources with new data from the residential and transportation sectors, Environ.
- 457 Sci. Technol., 51, 2821–2829, https://doi.org/10.1021/acs.est.6b03694, 2017.
- 458 Pan, Y., Tian, S., Liu, D., Fang, Y., Zhu, X., Gao, M., Wentworth, G. R., Michalski, G., Huang, X., and
- 459 Wang, Y.: Source apportionment of aerosol ammonium in an ammonia-rich atmosphere: an isotopic study
- 460 of summer clean and hazy days in urban beijing, J. Geophys. Res. Atmospheres, 123, 5681-5689,
- 461 https://doi.org/10.1029/2017JD028095, 2018.
- 462 Pan, Y., Gu, M., Song, L., Tian, S., Wu, D., Walters, W. W., Yu, X., Lü, X., Ni, X., Wang, Y., Cao, J., Liu,
- 463 X., Fang, Y., and Wang, Y.: Systematic low bias of passive samplers in characterizing nitrogen isotopic
- 464 composition of atmospheric ammonia, Atmospheric Res., 243, 105018-105025,
- 465 https://doi.org/10.1016/j.atmosres.2020.105018, 2020.
- 466 Qu, Q. and Zhang, K.: Effects of pH, total solids, temperature and storage duration on gas emissions
- 467 from slurry storage: a systematic review, Atmosphere, 12, 1156, https://doi.org/10.3390/atmos12091156,
- 468 2021.
- 469 Rosa, E., Arriaga, H., and Merino, P.: Ammonia emission from a manure-belt laying hen facility equipped
- 470 with an external manure drying tunnel, J. Clean. Prod., 251, 119591,
- 471 https://doi.org/10.1016/j.jclepro.2019.119591, 2020.
- 472 Savard, M. M., Cole, A., Smirnoff, A., and Vet, R.: δ 15 N values of atmospheric N species
- 473 simultaneously collected using sector-based samplers distant from sources isotopic inheritance and
- 474 fractionation, Atmos. Environ., 162, 11–22, https://doi.org/10.1016/j.atmosenv.2017.05.010, 2017.
- 475 Schlesinger, WilliamH. and Hartley, AnneE.: A global budget for atmospheric NH₃, Biogeochemistry, 15,
- 476 https://doi.org/10.1007/bf00002936, 1992.
- 477 Skinner, R., Ineson, P., Jones, H., Sleep, D., and Theobald, M.: Sampling systems for isotope-ratio mass
- 478 spectrometry of atmospheric ammonia, Rapid Commun. Mass Spectrom., 20, 81-88,
- 479 https://doi.org/10.1002/rcm.2279, 2006.





- 480 Soler-Jofra, A., Stevens, B., Hoekstra, M., Picioreanu, C., Sorokin, D., Van Loosdrecht, M. C. M., and
- 481 Pérez, J.: Importance of abiotic hydroxylamine conversion on nitrous oxide emissions during nitritation
- 482 of reject water, Chem. Eng. J., 287, 720–726, https://doi.org/10.1016/j.cej.2015.11.073, 2016.
- 483 Song, L., Walters, W. W., Pan, Y., Li, Z., Gu, M., Duan, Y., Lü, X., and Fang, Y.: 15N natural abundance
- 484 of vehicular exhaust ammonia, quantified by active sampling techniques, Atmos. Environ., 255, 118430-
- 485 118440, https://doi.org/10.1016/j.atmosenv.2021.118430, 2021.
- 486 Song, L., Wang, A., Li, Z., Kang, R., Walters, W. W., Pan, Y., Quan, Z., Huang, S., and Fang, Y.: Large
- 487 seasonal variation in nitrogen isotopic abundances of ammonia volatilized from a cropland ecosystem
- 488 and implications for regional NH₃ source partitioning, Environ. Sci. Technol., 58, 1177-1186,
- 489 https://doi.org/10.1021/acs.est.3c08800, 2024.
- 490 Stratton, J. J., Ham, J., Collett, J. L., Jr., Benedict, K., and Borch, T.: Assessing the efficacy of nitrogen
- 491 isotopes to distinguish colorado front range ammonia sources affecting rocky mountain national park,
- 492 Atmos. Environ., 215, https://doi.org/10.1016/j.atmosenv.2019.116881, 2019.
- 493 Streets, D. G., Bond, T. C., Carmichael, G. R., Fernandes, S. D., Fu, Q., He, D., Klimont, Z., Nelson, S.
- 494 M., Tsai, N. Y., Wang, M. Q., Woo, J.-H., and Yarber, K. F.: An inventory of gaseous and primary aerosol
- 495 emissions in Asia in the year 2000, J. Geophys. Res. Atmospheres, 108
- 496 https://doi.org/10.1029/2002JD003093, 2003.
- 497 Sui, Y., Ou, Y., Yan, B., Rousseau, A. N., Fang, Y., Geng, R., Wang, L., and Ye, N.: A dual isotopic
- 498 framework for identifying nitrate sources in surface runoff in a small agricultural watershed, northeast
- 499 China, J. Clean. Prod., 246, 119074, https://doi.org/10.1016/j.jclepro.2019.119074, 2020.
- 500 Ti, C., Gao, B., Luo, Y., Wang, X., Wang, S., and Yan, X.: Isotopic characterization of NH_X-N in
- deposition and major emission sources, Biogeochemistry, 138, 85–102, https://doi.org/10.1007/s10533-
- 502 018-0432-3, 2018.
- 503 Ti, C., Xia, L., Chang, S. X., and Yan, X.: Potential for mitigating global agricultural ammonia emission:
- 504 A meta-analysis, Environ. Pollut., 245, 141–148, https://doi.org/10.1016/j.envpol.2018.10.124, 2019.
- 505 Ti, C., Ma, S., Peng, L., Tao, L., Wang, X., Dong, W., Wang, L., and Yan, X.: Changes of δ15N values
- 506 during the volatilization process after applying urea on soil, Environ. Pollut., 270, 116204,
- 507 https://doi.org/10.1016/j.envpol.2020.116204, 2021.
- 508 Van Damme, M., Clarisse, L., Whitburn, S., Hadji-Lazaro, J., Hurtmans, D., Clerbaux, C., and Coheur,
- 509 P.-F.: Industrial and agricultural ammonia point sources exposed, Nature, 564, 99-103,
- 510 https://doi.org/10.1038/s41586-018-0747-1, 2018.
- 511 Walters, W. W., Karod, M., Willcocks, E., Baek, B. H., Blum, D. E., and Hastings, M. G.: Quantifying
- 512 the importance of vehicle ammonia emissions in an urban area of northeastern USA utilizing nitrogen
- 513 isotopes, Atmospheric Chem. Phys., 22, 13431-13448, https://doi.org/10.5194/acp-22-13431-2022,
- 514 2022.
- Wang, C., Yin, S., Bai, L., Zhang, X., Gu, X., Zhang, H., Lu, Q., and Zhang, R.: High-resolution ammonia





- 516 emission inventories with comprehensive analysis and evaluation in henan, china, 2006-2016, Atmos.
- 517 Environ., 193, 11–23, https://doi.org/10.1016/j.atmosenv.2018.08.063, 2018.
- 518 Wang, C., Li, X., Zhang, T., Tang, A., Cui, M., Liu, X., Ma, X., Zhang, Y., Liu, X., and Zheng, M.:
- 519 Developing nitrogen isotopic source profiles of atmospheric ammonia for source apportionment of
- 520 ammonia in urban beijing, Front. Environ. Sci., 10, https://doi.org/10.3389/fenvs.2022.903013, 2022.
- 521 Warner, J. X., Dickerson, R. R., Wei, Z., Strow, L. L., Wang, Y., and Liang, Q.: Increased atmospheric
- 522 ammonia over the world's major agricultural areas detected from space, Geophys. Res. Lett., 44, 2875-
- 523 2884, https://doi.org/10.1002/2016g1072305, 2017.
- 524 Wu, L., Ren, H., Wang, P., Chen, J., Fang, Y., Hu, W., Ren, L., Deng, J., Song, Y., Li, J., Sun, Y., Wang,
- 525 Z., Liu, C.-Q., Ying, Q., and Fu, P.: Aerosol ammonium in the urban boundary layer in beijing: insights
- from nitrogen isotope ratios and simulations in summer 2015, Environ. Sci. Technol. Lett., 6, 389–395,
- 527 https://doi.org/10.1021/acs.estlett.9b00328, 2019.
- 528 Wu, L., Zhang, Y., Xiao, Y., Zhu, J., Shi, Z., Wang, Y., Xu, H., Hu, W., Deng, J., Tang, M., and Fu, P.:
- 529 Diversity of ammonia sources in tianjin: nitrogen isotope analyses and simulations of aerosol ammonium,
- 530 Environ. Chem. 14482517, 21, 1–13, https://doi.org/10.1071/EN24030, 2024.
- 531 Xi, D., Xiao, Y., Mgelwa, A. S., and Kuang, Y.: Formation pathways and source apportionments of
- 532 inorganic nitrogen-containing aerosols in urban environment: insights from nitrogen and oxygen isotopic
- 533 compositions in guangzhou, china, Atmos. Environ., 309,
- 534 https://doi.org/10.1016/j.atmosenv.2023.119888, 2023.
- 535 Xiang, Y.-K., Dao, X., Gao, M., Lin, Y.-C., Cao, F., Yang, X.-Y., and Zhang, Y.-L.: Nitrogen isotope
- 536 characteristics and source apportionment of atmospheric ammonium in urban cities during a haze event
- 537 in northern China plain, Atmos. Environ., 269, 118800-118813,
- 538 https://doi.org/10.1016/j.atmosenv.2021.118800, 2022.
- 539 Xiao, H., Ding, S.-Y., Ji, C.-W., Li, Q.-K., and Li, X.-D.: Combustion related ammonia promotes PM2.5
- 540 accumulation in autumn in tianjin, china, Atmospheric Res., 275,
- 541 https://doi.org/10.1016/j.atmosres.2022.106225, 2022.
- Xiao, H., Xiao, H.-W., Xu, Y., Zheng, N.-J., and Xiao, H.-Y.: Combustion-driven inorganic nitrogen in
- 543 PM2.5 from a city in central china has the potential to enhance the nitrogen load of north China, J. Hazard.
- 544 Mater., 483, https://doi.org/10.1016/j.jhazmat.2024.136620, 2025.
- 545 Xiao, H.-W., Wu, J.-F., Luo, L., Liu, C., Xie, Y.-J., and Xiao, H.-Y.: Enhanced biomass burning as a
- 546 source of aerosol ammonium over cities in central China in autumn, Environ. Pollut., 266, 115278,
- 547 https://doi.org/10.1016/j.envpol.2020.115278, 2020.
- Xie, Y., Xiong, Z., Xing, G., Yan, X., Shi, S., Sun, G., and Zhu, Z.: Source of nitrogen in wet deposition
- 549 to a rice agroecosystem at tai lake region, Atmos. Environ., 42, 5182-5192,
- 550 https://doi.org/10.1016/j.atmosenv.2008.03.008, 2008.
- 551 Xu, P., Li, G., Zheng, Y., Fung, J. C. H., Chen, A., Zeng, Z., Shen, H., Hu, M., Mao, J., Zheng, Y., Cui,

https://doi.org/10.5194/egusphere-2025-4460 Preprint. Discussion started: 18 November 2025 © Author(s) 2025. CC BY 4.0 License.





- 552 X., Guo, Z., Chen, Y., Feng, L., He, S., Zhang, X., Lau, A. K. H., Tao, S., and Houlton, B. Z.: Fertilizer
- 553 management for global ammonia emission reduction, Nature, 626, 792-798,
- 554 https://doi.org/10.1038/s41586-024-07020-z, 2024.
- 555 Yang, F., Tan, J., Zhao, Q., Du, Z., He, K., Ma, Y., Duan, F., Chen, G., and Zhao, Q.: Characteristics of
- 556 PM_{2.5} speciation in representative megacities and across china, Atmospheric Chem. Phys., 11, 5207-
- 557 5219, https://doi.org/10.5194/acp-11-5207-2011, 2011.
- 558 Zhang, H., Hong, Z., Wei, L., Thornton, B., Hong, Y., Chen, J., and Zhang, X.: Stable isotopes unravel
- 559 the sources and transport of PM2.5 in the Yangtze River delta, china, Atmosphere, 14,
- 560 https://doi.org/10.3390/atmos14071120, 2023.
- 561 Zhang, L., Altabet, M. A., Wu, T., and Hadas, O.: Sensitive measurement of NH_4^+ 15N/14N ($\delta^{15}NH_4^+$) at
- 562 natural abundance levels in fresh and saltwaters, Anal. Chem., 79, 5297-5303,
- 563 https://doi.org/10.1021/ac070106d, 2007.
- 564 Zhou, Y., Zheng, N., Luo, L., Zhao, J., Qu, L., Guan, H., Xiao, H., Zhang, Z., Tian, J., and Xiao, H.:
- 565 Biomass burning related ammonia emissions promoted a self-amplifying loop in the urban environment
- 566 in kunming (SW china), Atmos. Environ., 253, https://doi.org/10.1016/j.atmosenv.2020.118138, 2021.
- 567 Zou, D., Sun, Q., Liu, J., Xu, C., and Song, S.: Seasonal source analysis of nitrogen and carbon aerosols
- 568 of PM2.5 in typical cities of zhejiang, china, Chemosphere, 303,
- 569 https://doi.org/10.1016/j.chemosphere.2022.135026, 2022.

570